

## Localized spatiotemporal chaos in surface waves

A. Kudrolli and J. P. Gollub

*Physics Department, Haverford College, Haverford, Pennsylvania 19041*

(Received 26 December 1995; revised manuscript received 10 April 1996)

A route to spatiotemporal chaos (STC) is identified in parametrically forced surface waves in which strongly disordered fluctuating domains coexist with textured stripes. The chaotic domains of this *mixed state* nucleate via instability at the most strongly curved regions of the stripe pattern. The area covered by the STC grows with the imposed acceleration, and fills all regions where the local curvature exceeds an  $\varepsilon$ -dependent critical curvature. The striped domains within the mixed state are also distorted by a secondary oscillatory instability at moderate viscosity. [S1063-651X(96)51808-8]

PACS number(s): 47.54.+r, 47.52.+j, 47.35.+i

The nature of spatiotemporal chaos (STC) in two-dimensional hydrodynamic systems has been explored in a number of experiments [1–5]. Although the disorder in STC is often relatively homogeneous spatially, there are also situations where it is localized. For example, in the “spiral turbulence” state of circular Couette flow between concentric cylinders, localized turbulent domains coexist with laminar regions [6]. Turbulent spots are also well known in shear turbulence [7]. Fluctuating localized disorder is sometimes termed spatiotemporal intermittency, and has been identified in several one-dimensional systems [8–10].

Surface waves induced through parametric instability by vertical forcing of the container (Faraday waves) are advantageous for studies of STC because the rapid time scale of the instability allows a multidimensional parameter space to be explored in a reasonable time. Furthermore, the strengths of nonlinear interactions between Fourier modes are a function of the excitation frequency [11]. A variety of phenomena related to STC have been reported in recent experiments, including spatiotemporal intermittency [12], spatial periodicity in temporally averaged patterns [13], and transverse amplitude modulations [14]. Instabilities and the onset of uniform STC were recently explored numerically using quasipotential model equations [15]. In previous experi-

ments, persistent spatial inhomogeneities did not occur. However, these studies were limited by a relatively modest aspect ratio  $\Gamma$  (the ratio of the cell width or diameter  $D$  to half the wavelength). Here we describe phenomena obtained in a particularly large apparatus providing relatively high  $\Gamma$  (up to 100 at the frequencies of interest here). Furthermore, high driving accelerations (up to 15g) allow high viscosity fluids to be studied, where boundary effects are less significant, and the initial patterns are textured stripes (nearly one-dimensional standing waves) comparable to the rolls found in convection experiments.

We discovered several phenomena in a systematic survey of the primary and secondary instabilities as a function of the driving frequency and the viscosity  $\nu$ . Here we focus on a surprising type of transition to STC in which localized and strongly fluctuating disordered domains *coexist* with laminar stripes (see Fig. 1). The persistent disordered domains of this “mixed state” have an  $\varepsilon$ -dependent critical curvature at their boundary. The stripes within the mixed state can also be deformed by an additional oscillatory instability.

The experiments are conducted using a circular container 32 cm in diameter, and a fluid layer 0.3 cm deep. The rigid temperature-controlled Delrin container is driven vertically with single frequency sinusoidal forcing at frequency  $f_0$ , us-

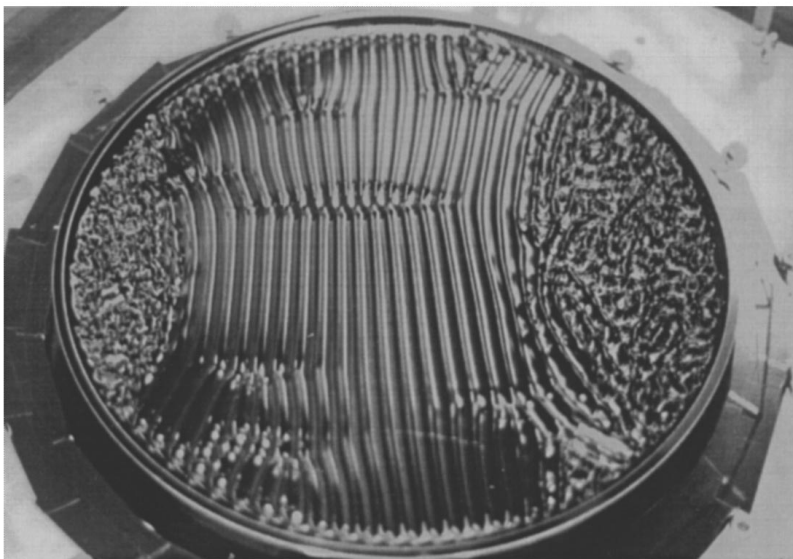


FIG. 1. Photograph (inclined view) of the mixed state, in which domains of textured stripes and spatiotemporal chaos coexist ( $\nu=1.0 \text{ cm}^2\text{s}^{-1}$ ;  $f_0=45 \text{ Hz}$ ;  $\varepsilon=0.45$ ). The wave amplitudes in the chaotic domains are much larger than in the striped domains.

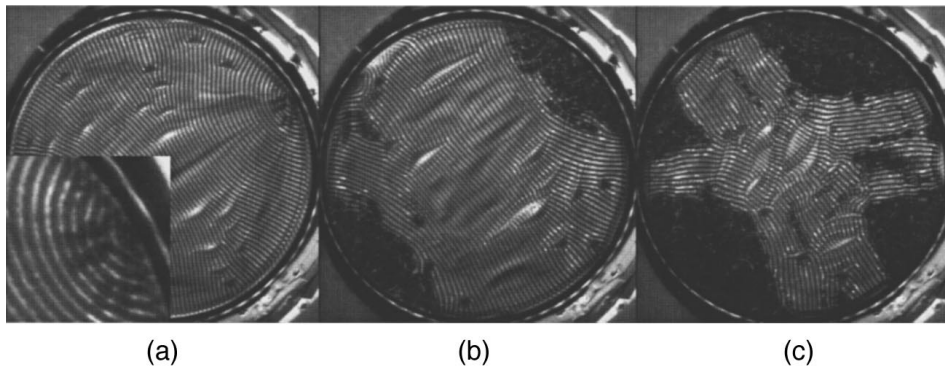


FIG. 2. Wave patterns as a function of driving amplitude. (The driving frequency  $f_0=45$  Hz, and the kinematic viscosity  $\nu=1.0$  cm<sup>2</sup>s<sup>-1</sup>.) (a) Dimensionless acceleration  $\varepsilon=0.21$ : transverse amplitude modulations develop near the focus singularities of the stripes (see inset). (b)  $\varepsilon=0.43$  and (c)  $\varepsilon=0.61$ : strong spatiotemporal chaos develops in the high curvature regions and spreads with increasing  $\varepsilon$ .

ing a massive electromagnetic shaker capable of peak forces of 2200 N. The driving frequency can be varied over the range 10–200 Hz. The measured spatial inhomogeneity of the driving acceleration is  $\pm 2\%$ . Previous experiments using this apparatus have given excellent agreement with linear instability theory for the primary instability over a wide range of frequency and viscosity [16]. A circularly symmetric ring of lights illuminates the container; reflected light is collected by a  $512 \times 512$  pixel charge coupled device (CCD) camera at the center of the ring. Bright intensities in the images correspond to antinodes, and dark ones to nodes. Further details can be found in Ref. [16].

In Fig. 2, a sequence of images shows the transition to a mixed state where regions of STC coexist with textured stripes for silicone oil with kinematic viscosity  $\nu=1$  cm<sup>2</sup>s<sup>-1</sup>. We define the control parameter  $\varepsilon$  conventionally as  $\varepsilon=(a-a_c)/a_c$ , where  $a_c$  is the acceleration at the primary instability. The patterns are allowed to reach a steady state after each small increment in  $\varepsilon$ , starting from  $\varepsilon<0$ . Striped patterns are formed initially with two focus singularities developing at the container boundary, and with the stripes aligned roughly perpendicular to the boundary. When the driving amplitude is increased, transverse amplitude modulations (TAM's) [17,18] are observed to form near the focus singularities [see Fig. 2(a) and the inset].

The amplitude of these modulations increases sharply with the driving amplitude; this growth leads to the formation of defects. Over an interval of only about 3% in acceleration, the growing amplitude modulations destroy the phase coherence of the stripes. They are locally replaced by a disordered, relatively isotropic, and strongly fluctuating structure. Figures 1 and 2(b) show this *mixed state* where domains of STC coexist with other regions of textured stripes. The wave amplitude in the STC domains is much higher than that in the striped regions, and the surface there resembles an irregular array of columns, with amplitudes *exceeding* the wavelength. The STC domains scatter light at large angles, and hence appear dark in Fig. 2(b). Droplets are occasionally ejected from the STC domains. (Droplet ejection has recently been investigated experimentally [19] at much lower  $\nu$ .)

The domains of STC grow with increasing  $\varepsilon$ , as shown in Fig. 2(c). The boundary separating the STC and striped regions is well defined, and the amplitude difference quite large (several mm typically). The boundary itself can also evolve, but only over times much longer than the time scale for fluctuations within the STC domains, which is comparable to the *wave period*. It is interesting to note that the STC

domains develop in regions that had high curvature at lower  $\varepsilon$ .

The phase diagram of the patterns as a function of driving frequency  $f_0$  and acceleration  $a/g$  is shown in Fig. 3 for  $\nu=1.0$  cm<sup>2</sup>s<sup>-1</sup>. Textured stripes similar to Fig. 2(a) occur near onset for  $f_0 \geq 40$  Hz. As  $f_0$  is reduced, the stripes become shorter, and the resulting defects lead to time dependence even near onset. The TAM transition and the mixed state described in the previous paragraphs are most cleanly observed for  $f_0 \geq 40$  Hz. For  $f_0 < 20$  Hz, hexagons are observed near onset as in some previous experiments ([20,21]), but we find them over a much broader range of viscosities. We also note that hexagonal states extend to progressively higher frequencies as  $\nu$  is reduced. A theory that may be applicable at the lower viscosities has been given recently by Zhang [11].

To test the importance of curvature in the initiation of the STC domains, and the dependence of the mixed state on the manner in which it is produced, the acceleration was increased suddenly from a value below onset in a discontinuous step. The instability occurs first at the boundary and the resulting stripes then extend to the center, where a focus singularity forms. If  $\varepsilon$  is sufficiently high, a circular domain of STC is nucleated at the center and evolves over a few seconds to a quasisteady radius as shown in Fig. 4. However,

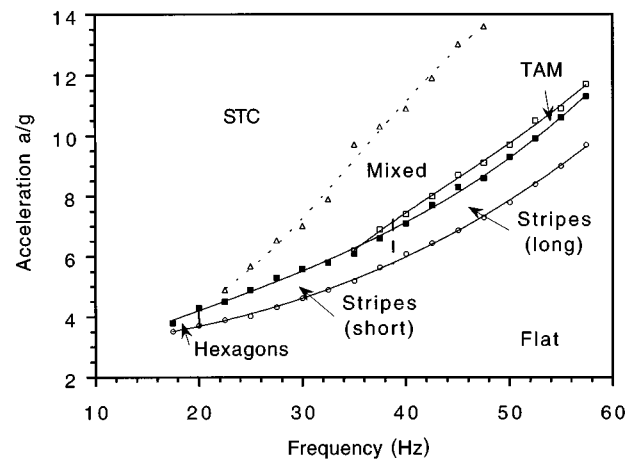


FIG. 3. Phase diagram showing the patterns observed as a function of  $f_0$  and acceleration  $a/g$  for  $\nu=1.0$  cm<sup>2</sup>s<sup>-1</sup>. The ‘‘mixed’’ state is shown in Fig. 1; in the region denoted STC, chaotic domains fill the entire cell. The transverse amplitude modulations (TAM's) are described in the text.

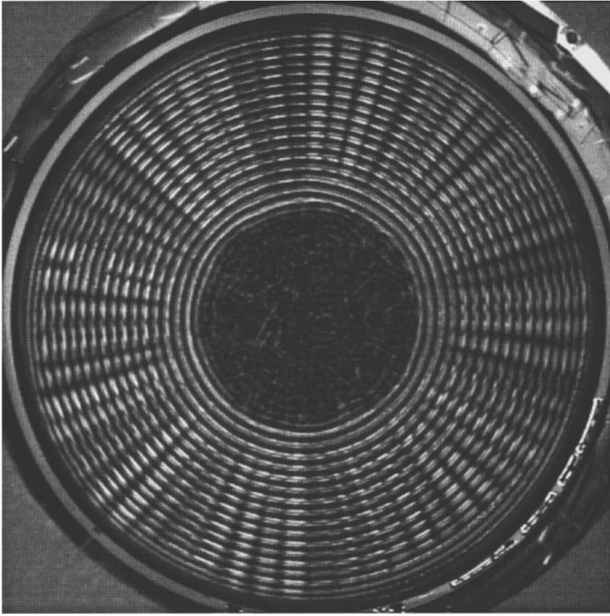


FIG. 4. Transient pattern induced after  $\varepsilon$  is stepped suddenly from below threshold ( $\varepsilon < 0$ ) to  $\varepsilon = 0.42$  at time  $t = 0$ , for  $f_0 = 40$  Hz. The STC domain in the middle of the cell at  $t = 3$  s. (The azimuthal intensity variations are due to discreteness of the ring of 58 lights.) The pattern soon suffers a large scale instability and the chaotic domain eventually moves toward the boundary as in Fig. 2(b).

the stripes are not stable in this configuration. The stripes evolve to become more nearly normal to the boundaries over a time of about 300 s, and the STC domains are carried to the boundaries. The resulting mixed state is essentially indistinguishable from those produced when the driving amplitude is increased slowly [Fig. 2(b)]. This sequence of phenomena is qualitatively reproducible over a substantial range of  $\varepsilon$  and  $f_0$ . It demonstrates that the mixed state is not a result of spatial inhomogeneities in  $a$ , and that the STC domains always occur in the high curvature regions of the stripes.

The size of the initial circular chaotic region depends on  $\varepsilon$ . The fraction of the container surface covered by the STC domains is a useful measure to characterize the mixed state. This quantity is plotted in Fig. 5(a) as a function of  $\varepsilon$  for both the transient circular domains (squares), and the case of slowly augmenting  $a$  (circles). The two cases are consistent to within the experimental uncertainty; there is also no evidence of hysteresis. The data shown are for a driving frequency of 45 Hz, but are representative of data obtained anywhere in the region where the primary pattern consists of long stripes. The TAM instability (and the onset of the mixed state) is seen to occur near  $\varepsilon = 0.2$ , with little frequency dependence. The STC fraction increases smoothly, until at  $\varepsilon = 0.9$ , the whole cell becomes chaotic.

In Fig. 5(b) the radius of curvature of the boundary that separates the STC and striped domains is plotted as a function of  $\varepsilon$ . For the case of slowly augmented  $\varepsilon$  (circles) this *critical curvature* decreases with increasing  $\varepsilon$  and approaches zero at high  $\varepsilon$ , where the boundary is nearly straight. For the circular transient STC domains, the critical curvature also falls, but the decline is not identical and can be followed only up to  $\varepsilon = 0.6$  because the shape of the initial domain becomes irregular.

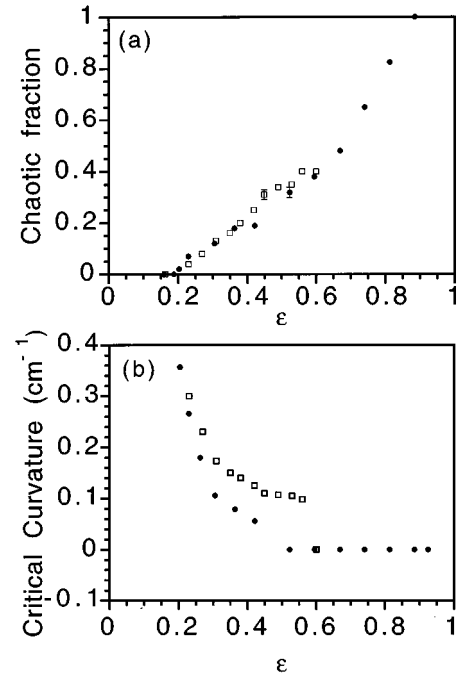


FIG. 5. (a) Chaotic fraction in the mixed state as a function of  $\varepsilon$ . (b) Critical curvature (at the edge of the chaotic domains) as a function of  $\varepsilon$ . The circles correspond to changing  $\varepsilon$  very slowly for  $f_0 = 45$  Hz as in Fig. 2, and the squares to data obtained just after a sudden transition is induced as in Fig. 4.

It is interesting to speculate as to why the STC domains are confined to the high curvature regions near the onset of the secondary instability. Wave number variations *do not* seem to be primarily responsible for the local instability. The wave number in the unstable region varies by about  $\pm 7\%$  both above and below that in the center of the pattern, depending on the direction of displacement from the focus singularity. Therefore, we believe that curvature (and  $\varepsilon$ ), not wave number, are the two parameters defining the threshold for the STC domains.

A qualitatively similar phase diagram was obtained for a lower viscosity ( $\nu = 0.5 \text{ cm}^2 \text{ s}^{-1}$ ) silicone oil, including the mixed state. However, there are some differences. Square patterns occur at intermediate frequencies along with hexagons and stripes. Transverse amplitude modulations are visible over the entire cell before they initiate defects leading to STC at the focus singularities. Finally, the STC domain boundaries are somewhat more diffuse at lower  $\nu$ . Possible explanations for the more diffuse boundaries are that (a) the correlation length increases with decreasing  $\nu$ , and (b) the curvature of the stripes near the focus singularities is less at lower  $\nu$ .

The ordered stripes within the mixed state can experience additional secondary instabilities. For example, an oscillatory instability occurs in conjunction with the mixed state for  $\nu$  near  $0.5 \text{ cm}^2 \text{ s}^{-1}$ , as shown in Fig. 6. This picture is an average over one period of the primary waves. The deformations are primarily standing transverse waves on the striped pattern, with a temporal period of a few wave periods; the deformations also travel slowly along the stripes, possibly due to amplitude mismatch between the two components of the standing wave. The wavelength parallel to the stripes is

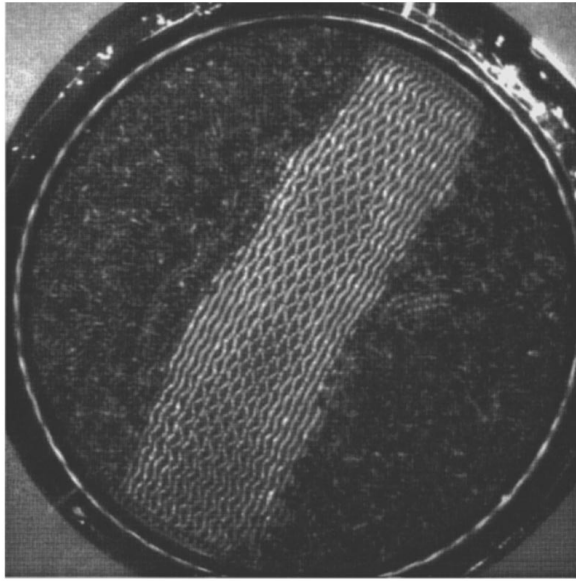


FIG. 6. Oscillatory instability of the stripe pattern in the mixed state for  $\nu=0.5 \text{ cm}^2\text{s}^{-1}$ . ( $f_0=45 \text{ Hz}$ , and  $\varepsilon=0.95$ .)

of the same order as the basic hydrodynamic wavelength but varies by 20% over the pattern. The deformations are somewhat intermittent, and the phase relationships between adjacent stripe boundaries vary from one part of the pattern to another. This oscillatory instability resembles the oscillatory instability of thermal convection rolls [22,23]. It is quite different from the TAM instability, a traveling modulation of wave *amplitude* that does not deform the stripes laterally.

A mixed state with persistent localized STC domains appears to occur only for the striped patterns. Although the TAM instability was seen for the square patterns (at lower

$\nu$ ), the mixed state was *not* observed in that regime. For parameters giving rise to hexagonal primary states (at lower driving frequencies), STC develops relatively uniformly but continuously across the container as the hexagonal lattice becomes disordered orientationally [24]. Thus, the transition to STC is strongly dependent on the symmetry of the primary pattern.

In conclusion, we have demonstrated the existence of a *mixed state* for parametrically forced surface waves in which strong spatiotemporal chaos and laminar stripes (nearly one-dimensional standing waves) coexist. The dynamics of this state can be largely understood in terms of an  $\varepsilon$ -dependent critical curvature of the stripes. The phenomenon is not a consequence of a particular cell geometry (foci occur for any container geometry) and is expected to persist for even larger  $\Gamma$  (larger  $f_0$  or  $D$ ). Experimentally, we find that increasing  $f_0$  (up to 70 Hz) does not affect the stripe curvature at a given distance from the foci. Further increases in  $f_0$  or  $D$  are impractical, but it is clear that the structure near the foci would be nearly the same, so that localized domains of STC are still expected.

It remains to be seen whether the dynamics of these mixed domain patterns (especially the role of stripe curvature in promoting instability) can be incorporated into an appropriate set of amplitude equations, and whether similar phenomena occur in other systems with stripe or roll patterns. A systematic study of the various primary patterns and routes to spatiotemporal chaos as a function of viscosity and frequency will appear elsewhere [24].

W.S. Edwards designed the apparatus and control systems used for these investigations and B. Boyes provided technical support. We appreciate helpful discussions with M.C. Cross, H. Riecke, and W. Zhang. This work was supported by NSF Grant No. DMR-9319973.

- 
- [1] For a review, see M. C. Cross and P. C. Hohenberg, *Rev. Mod. Phys.* **65**, 851 (1993).
- [2] Y. Hu, R. E. Ecke, and G. Ahlers, *Phys. Rev. Lett.* **74**, 5040 (1995).
- [3] S. W. Morris, E. Bodenschatz, D. S. Cannell, and G. Ahlers, *Phys. Rev. Lett.* **71**, 2026 (1993).
- [4] N. B. Tufillaro, R. Ramshankar, and J. P. Gollub, *Phys. Rev. Lett.* **62**, 422 (1989).
- [5] I. Rehberg, S. Rasenat, and V. Steinberg, *Phys. Rev. Lett.* **62**, 756 (1989).
- [6] J. J. Hegseth, C. D. Andereck, F. Hayot, and Y. Pomeau, *Phys. Rev. Lett.* **62**, 257 (1989).
- [7] F. Daviaud, J. Hegseth, and P. Bergé, *Phys. Rev. Lett.* **69**, 2511 (1992).
- [8] S. Michalland, M. Rabaud, and Y. Couder, *Europhys. Lett.* **22**, 17 (1993).
- [9] F. Melo and S. Douady, *Phys. Rev. Lett.* **71**, 3283 (1993).
- [10] S. Ciliberto and P. Bigazzi, *Phys. Rev. Lett.* **60**, 286 (1988).
- [11] W. Zhang, Ph.D. dissertation, Florida State University, 1994 (unpublished).
- [12] E. Bosch and W. van de Water, *Phys. Rev. Lett.* **70**, 3420 (1993).
- [13] B. J. Gluckman, P. Marcq, J. Bridger, and J. P. Gollub, *Phys. Rev. Lett.* **71**, 2034 (1993).
- [14] L. Daudet, V. Ego, S. Manneville, and J. Bechhoefer, *Europhys. Lett.* **32**, 313 (1995).
- [15] W. Zhang and J. Viñals, *Phys. Rev. Lett.* **74**, 690 (1995).
- [16] T. Besson, W. S. Edwards and L. S. Tuckerman (unpublished).
- [17] S. T. Milner, *J. Fluid Mech.* **225**, 81 (1991).
- [18] In smaller square cells, the TAM instability has been observed over the entire cell. See Ref. [14].
- [19] C. L. Goodridge, W. T. Shi, and D. P. Lathrop, *Phys. Rev. Lett.* **76**, 1824 (1996).
- [20] B. Christiansen, P. Alstrom, and M. T. Levinsen, *Phys. Rev. Lett.* **68**, 2157 (1992).
- [21] K. Kumar and K. M. S. Bajaj, *Phys. Rev. E* **52**, R4606 (1995).
- [22] F. H. Busse and J. A. Whitehead, *J. Fluid Mech.* **47**, 305 (1971).
- [23] V. Croquette and H. Williams, *Physica D* **37**, 300 (1989).
- [24] A. Kudrolli and J. P. Gollub (unpublished).